



ELSEVIER

Contents lists available at SciVerse ScienceDirect

# Nuclear Instruments and Methods in Physics Research A

journal homepage: [www.elsevier.com/locate/nima](http://www.elsevier.com/locate/nima)

## Radon removal from gaseous xenon with activated charcoal

K. Abe<sup>a</sup>, K. Hieda<sup>a</sup>, K. Hiraide<sup>a</sup>, S. Hirano<sup>a</sup>, Y. Kishimoto<sup>a</sup>, K. Kobayashi<sup>a</sup>, Y. Koshio<sup>a</sup>, J. Liu<sup>b</sup>, K. Martens<sup>b</sup>, S. Moriyama<sup>a</sup>, M. Nakahata<sup>a,b</sup>, H. Nishiie<sup>a</sup>, H. Ogawa<sup>a</sup>, H. Sekiya<sup>a</sup>, A. Shinozaki<sup>a</sup>, Y. Suzuki<sup>a,b</sup>, O. Takachio<sup>a</sup>, A. Takeda<sup>a</sup>, K. Ueshima<sup>a</sup>, D. Umemoto<sup>a</sup>, M. Yamashita<sup>a</sup>, K. Hosokawa<sup>c</sup>, A. Murata<sup>c</sup>, K. Otsuka<sup>c</sup>, Y. Takeuchi<sup>c</sup>, F. Kusaba<sup>e</sup>, D. Motoki<sup>d,\*</sup>, K. Nishijima<sup>e</sup>, S. Tasaka<sup>f</sup>, K. Fujii<sup>g</sup>, I. Murayama<sup>g</sup>, S. Nakamura<sup>g</sup>, Y. Fukuda<sup>h</sup>, Y. Itow<sup>i</sup>, K. Masuda<sup>i</sup>, Y. Nishitani<sup>i</sup>, H. Takiya<sup>i</sup>, H. Uchida<sup>i</sup>, Y.D. Kim<sup>j</sup>, Y.H. Kim<sup>k</sup>, K.B. Lee<sup>k</sup>, M.K. Lee<sup>k</sup>, J.S. Lee<sup>k</sup>

<sup>a</sup> Kamioka Observatory, Institute for Cosmic Ray Research, The University of Tokyo, Kamioka, Hida, Gifu 506-1205, Japan

<sup>b</sup> Institute for the Physics and Mathematics of the Universe, The University of Tokyo, Kashiwa, Chiba 277-8582, Japan

<sup>c</sup> Department of Physics, Kobe University, Kobe, Hyogo 657-8501, Japan

<sup>d</sup> School of Science and Technology, Tokai University, Hiratsuka, Kanagawa 25 9-1292, Japan

<sup>e</sup> Department of Physics, Tokai University, Hiratsuka, Kanagawa 25 9-1292, Japan

<sup>f</sup> Department of Physics, Gifu University, Gifu, Gifu 501-1193, Japan

<sup>g</sup> Department of Physics, Faculty of Engineering, Yokohama National University, Yokohama, Kanagawa 240-8501, Japan

<sup>h</sup> Department of Physics, Miyagi University of Education, Sendai, Miyagi 980-0845, Japan

<sup>i</sup> Solar Terrestrial Environment Laboratory, Nagoya University, Nagoya, Aichi 464-8602, Japan

<sup>j</sup> Department of Physics, Sejong University, Seoul 143-747, South Korea

<sup>k</sup> Korea Research Institute of Standards and Science, Daejeon 305-340, South Korea

## The XMASS Collaboration

### ARTICLE INFO

#### Article history:

Received 29 August 2011

Received in revised form

23 September 2011

Accepted 28 September 2011

Available online 8 October 2011

#### Keywords:

Radon

Xenon

Charcoal

### ABSTRACT

Many low background experiments using xenon need to remove radioactive radon to improve their sensitivities. However, no method of continually removing radon from xenon has been described in the literature. We studied a method to remove radon from xenon gas through an activated charcoal trap. From our measurements we infer a linear relationship between the mean propagation velocity  $v_{Rn}$  of radon and  $v_{Xe}$  of xenon in the trap with  $v_{Rn}/v_{Xe} = (0.96 \pm 0.10) \times 10^{-3}$  at  $-85^\circ\text{C}$ . As the mechanism for radon removal in this charcoal trap is its decay, knowledge of this parameter allows us to design an efficient radon removal system for the XMASS experiment. The verification of this system found that it reduces radon by a factor of 0.07, which is in line with its expected average retention time of 14.8 days for radon.

© 2011 Elsevier B.V. All rights reserved.

## 1. Introduction

Liquid noble gases are increasingly used in low background experiments due to both their high purity and good performance as a radiation detector. Xenon (Xe) is a particularly attractive candidate, as it has the highest mass number, produces scintillation light in the range of typical photomultiplier (PMT) sensitivities, and has no long lived radioactive isotopes of its own [1–3]. The XMASS experiment at the Kamioka Observatory in Japan uses liquid Xe (LXe) to search for possible WIMP Dark Matter recoils. It uses especially developed low radioactivity PMTs to measure the

scintillation light from nuclear and other recoils in its LXe volume. The high scintillation light yield of LXe (comparable to that of NaI(Tl)) allows for good energy resolution and a low detection threshold. Its high density and lack of radioactive isotopes provide excellent shielding against background radiation from without as well as within the detector [4]. The sensitivity of the XMASS experiment is expected to be better than  $10^{-45} \text{ cm}^2$  for a dark matter particle mass of  $100 \text{ GeV}/c^2$  with 100 kg effective volume and 5 years exposure time. As the power dispersed by the PMTs submerged in the LXe naturally leads to continuous evaporation of liquid from above the detector itself, both liquid and gas phase circulation are part of the XMASS detector design and can be used to maintain the purity of the detector medium, the LXe.

Thanks to the short half-life times of all its radioactive isotopes chemically pure Xe does not have any intrinsic radioactivity.

\* Corresponding author.

E-mail address: [motoki@tkikam.sp.u-tokai.ac.jp](mailto:motoki@tkikam.sp.u-tokai.ac.jp) (D. Motoki).

While efficient means exist to remove admixtures other than noble gases, trace admixtures of in particular krypton (Kr) and radon (Rn) with their respective radioactive isotopes and decay chains have to be taken care of separately.  $^{85}\text{Kr}$  (10.756 yr) and  $^{222}\text{Rn}$  (3.82 day), Rn's longest lived isotope, are of particular concern. While in XMASS Kr was removed by distillation [5] prior to filling the LXe into the detector,  $^{222}\text{Rn}$  is a daughter of  $^{238}\text{U}$  and will be re-supplied continuously from the uranium decay chain in the structural elements of any type of detector. Some of the emanating Rn will inevitably decay in the effective volume of the detector. Self-shielding therefore does not help to reduce this background, and Rn in the LXe detector medium will have to be reduced to an acceptable level continually throughout the lifetime of the experiment.

As both Rn and Xe are chemically inert noble gases, one is reduced to exploiting small physical differences between the two elements. Activated charcoal is an effective adsorbent for various impurities by physical adsorption. Its adsorption of some rare gases was investigated in [6]. In Kamioka the Super-Kamiokande group is using activated charcoal to produce Rn free air [7]. Rn adsorption in argon gas was confirmed in [8], and the mechanism of adsorption in charcoal was discussed in [9,10]. However, it can be expected to be difficult to remove Rn from Xe as atomic size of Xe and Rn is not very different; parameters that govern the adsorption of materials in the pores of different charcoal samples. The charcoal used in the XMASS experiment and throughout all of our measurements reported in this paper was Shirasagi G<sub>2X</sub> 4/6, which is a product of Japan EnviroChemicals, Ltd. The charcoal has cylindrical shape, and its grain size is 4.75 ~ 3.36 mm. It was selected from a range of products measured by High-Purity Germanium detector produced by CANBERRA, it had the lowest contamination with radium ( $0.067 \pm 0.015$  mBq/g), of which Rn is a daughter.

Activated charcoal traps (hereafter simply referred to as charcoal traps or traps) can be understood as an analog to columns in gas chromatography. In this paper we consistently interpret our measurements in terms of different propagation speeds for Rn and Xe in our charcoal traps. If a given charcoal trap is long enough so that Rn moving at its measured propagation speed needs a couple of Rn lifetimes before it emerges again at the other end of the trap, the appropriate portion of it will have decayed naturally and the overall Rn concentration in the Xe carrier gas moving through the trap is reduced by that amount. The measured parameters are therefore used to design an appropriate system to continually remove radon from the LXe used as detector medium in the XMASS experiment, and we verified that this system performs according to expectations.

This paper is organized in four sections, including this introduction. In section two we describe experiments designed to verify the system parameters relevant to radon removal from gaseous Xe in charcoal traps. These findings are applied to the design of a dedicated Rn removal system for XMASS in section three. In this section we also report measurements we made to ascertain this system's performance. The final section offers our conclusions.

## 2. Rn removal from Xe gas: measurements

### 2.1. The experimental setup

The following experiments were designed to verify the concept of a Rn propagation speed  $v_{Rn}$  for Rn progression through the charcoal trap that would be sufficiently lower than the average speed  $v_{Xe}$  of the bulk Xe component to allow efficient removal of the radioactive Rn contaminant through its natural decay. While

$v_{Xe}$  in the trap is easily obtained as the ratio of overall flow through the trap  $f_{Xe}$  to the cross-sectional area  $A_{trap}$  of the trap,  $v_{Rn}$  needs to be extracted from the temporal evolution of the Rn concentration after the carrier gas (Xe) is passed through the trap. In particular that requires to be able to inject a measurable amount of Rn into the system and have a reliable means of monitoring the concentration of Rn in the system.

The first problem of injecting a measurable quantity of Rn into our Xe carrier gas is easily solved with a commercial Rn gas source (Pylon RNC Calibrated Radon Gas Source; Ra-226). With regard to the second problem there fortunately is a lot of expertise available at the Kamioka Observatory. We employed a PIN photodiode based electrostatic collection type Rn detector with a 70 l volume [11]. This detector identifies decays of the Rn daughters  $^{218}\text{Po}$  and  $^{214}\text{Po}$  collected onto its photodiode by measuring the energy of their respective emitted alpha particles. Given their distinctive alpha energies both isotopes can thus be monitored independently. While  $^{214}\text{Po}$  has a higher collection efficiency in the electrostatic field leading it to the photodiode, it also has a longer lifetime that requires longer measurements and implies a larger time lag. For this reason we mainly analyzed the  $^{218}\text{Po}$  data to measure Rn concentration. To monitor the Rn concentration we integrate the respective  $^{218}\text{Po}$  counts over 10 min intervals and use calibrated efficiencies to obtain the averaged Rn concentration for the respective 10 min interval.

The layout of our system is shown on the left hand side of Fig. 1. The two main parts were the aforementioned Rn detector and the charcoal trap. The trap was usually immersed in a coolant reservoir to keep its temperature stable at  $-85^\circ\text{C}$ . It also was fitted with a heating mechanism which allowed us to bake the trap at  $120^\circ\text{C}$ . As our measurements showed, this temperature was sufficiently high to release all previously adsorbed Rn. The charcoal trap can be isolated from the rest of the system while circulation would be maintained by means of a bypass to the trap. The same is true for the getter [12] that can be used to remove contaminants other than Rn from the Xe, and the aforementioned Rn source. The bypass to the circulation pump was mostly adjusted just to arrange for conditions that would allow the Xe calibrated mass flow controller to maintain the desired flow rate through the circulation system. Not shown in the diagram are the Xe supply system and a vacuum station that allows to evacuate the whole system.

In preparation for a measurement cycle the system was evacuated, and the charcoal trap was first baked under vacuum. Next the system was filled with Xe gas and circulation was started while we were still baking the charcoal trap. At this point the circulation included all components except for the Rn source. The pressure was almost atmospheric pressure. Due to the charcoal adsorption, it moved from 0.09 to 0.12 MPa when we used three charcoal traps. In particular the getter was always kept in the system during all circulation to keep the dew point  $< -70^\circ\text{C}$ . While still baking it the charcoal trap was then isolated from the rest of the circulation system by switching circulation to the bypass for the trap. In isolation, the trap was cooled down from its baking temperature of  $120^\circ\text{C}$  to its operating temperature of  $-85^\circ\text{C}$ , which is coolant temperature. During this cooling process Xe itself got adsorbed in the trap and the pressure in the trap dropped accordingly. Next Rn was injected into the circulation system from the Rn source while circulation continued through the Rn detector and the getter. After Rn injection the measurement cycle started with a measurement of the newly attained Rn concentration in the circulation system. After some section of the Rn decay curve was measured and the trap had reached its operating temperature, the Xe flow was switched from the bypass to go through the trap. This was done under the control of the mass flow meter by first opening only the inlet side of the trap

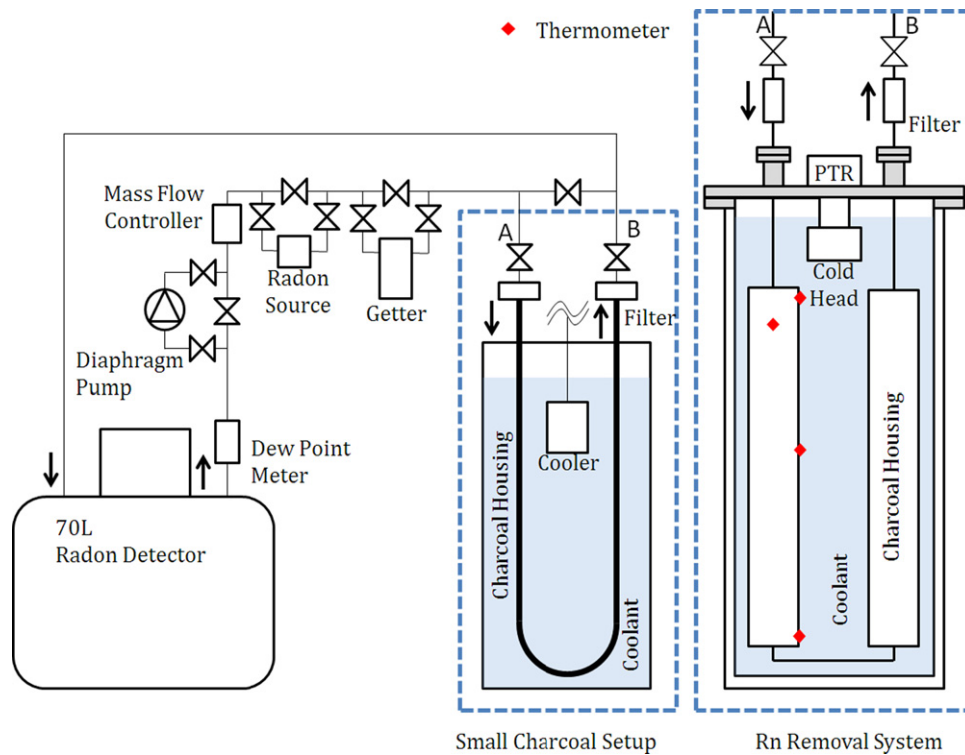


**Fig. 1.** Layout of the Xe circulation and Rn concentration measurement system. The charcoal traps are connected at points A and B. The right side of the figure shows the layout of the newly designed charcoal trap for XMASS with the location of its temperature sensors, which was also tested in the left side system.

until the pressure in the cold trap became too high to maintain the desired flow rate; at this point the outlet side of the trap was opened too to allow continuous circulation through the trap. Circulating through the charcoal trap the system ultimately settles into a new and lower equilibrium concentration for Rn in the Xe carrier gas. Once this new equilibrium concentration is reached and our measurements traced the Rn decay curve again for a suitable amount of time at the new lower level, cooling is removed from the trap and the trap is baked once again to restore the trapped Rn to the system. That the ensuing rise in the measured Rn concentration always recovered the decay curve originally measured right after Rn filling is proof that the Rn that had been removed while operating the trap at low temperature really had been adsorbed in the charcoal. Circulation through the trap was continuing throughout this radon release phase of the measurement. A new measurement cycle may have been started without adding new Rn by simply isolating the baking trap again to cool it down during bypass circulation. One measurement cycle therefore consists of three different phases: bypass circulation, trapping circulation, and release circulation.

As mentioned before the parameters we want to control in our system are the overall flow rate  $f_{Xe}$  as well as length  $L_{trap}$  and cross-sectional area  $A_{trap}$  of the trap itself. Control of  $L_{trap}$  and  $A_{trap}$  was achieved by simply preparing three identical sections of charcoal trap that in a sequence of experiments were then installed either in sequence or in parallel, doubling or tripling either the length (sequence) or the area (parallel) of the trap. One such charcoal section had a length of 174 cm and a cross-section of  $0.94 \text{ cm}^2$ , containing 58.6 g of activated charcoal. The tube itself was cut from standard 1/2 in. copper tubing.

## 2.2. Extracting the Rn propagation velocity in the trap

**Fig. 2** shows the results of a sequence of measurement cycles made after one Rn injection and with all three traps arranged in

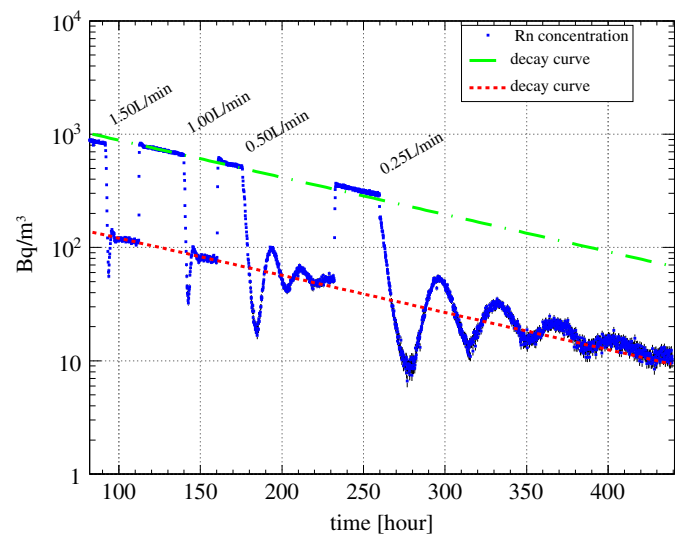


**Fig. 2.** Rn concentration measurements for a sequence of Rn trapping experiments with three charcoal traps installed in series. The data points for four Rn release and trapping sequences at different Xe flow rates are shown together with  $^{222}\text{Rn}$  decay curves fitted to the Rn released and trapped equilibrium states of the system. Data points are derived from the count rates for  $^{218}\text{Po}$  accumulated over 10 min.

series, resulting in  $L_{trap} = 522 \text{ cm}$  and  $A_{trap} = 0.94 \text{ cm}^2$  with a total of 175.8 g of charcoal for these measurements. Note that between measurement cycles bypass circulation is always necessary in order to allow the cooling down of the charcoal trap without starting to trap radon from the reservoir in the 70 l Rn detector prematurely.

The data points in this figure show the  $^{222}\text{Rn}$  concentration in  $[\text{Bq}/\text{m}^3]$  as measured in the Rn detector by  $^{218}\text{Po}$  counts.  $f_{Xe}$  was different for each measurement cycle and is indicated in the figure. The figure also shows two decay curves with the proper

$^{222}\text{Rn}$  lifetime fit to the data; the upper dash-dotted one shows the temporal evolution of the injected Rn concentration when no Rn is trapped in the charcoal (baking condition) and the lower dotted one the temporal evolution of the equilibrium concentration of Rn in the system when the traps are cooled to operating temperature.

Two important conclusions of all our measurements are immediately evident from this figure. First: for flow rates between 0.25 and 1.50 l/min the equilibrium Rn concentration as a fraction of the injected Rn concentration (adjusted for natural decay) after Rn adsorption in the traps is independent of the overall flow rate through the traps. Second: baking at the end of the cycle releases all the adsorbed Rn from the trap, and the original Rn concentration (adjusted for natural decay) is restored. As mentioned before this is also evidence that Rn really was adsorbed in the cooled traps.

To interpret our measurements we invoke the analogy with gas chromatography again. Our setup is best understood as consisting of one mixing reservoir (the 70 l Rn detector) and one delay line (the charcoal trap). Mixing in the reservoir takes place between the output of the delay line and the contents of the reservoir, which are simultaneously fed into the delay line. At the beginning of a measurement cycle the trap is empty and Rn loaded Xe enters the delay line. But because of the delay – here is where the analogy with gas chromatography becomes relevant – no Rn appears at the output yet. The Rn concentration in the reservoir drops as essentially Rn free Xe leaves the trap to dilute the Rn concentration in the reservoir. Since at 1.00 l/min the volume of the detector is turned over in a little over 1 h, the Rn concentration in the reservoir (the Rn detector) drops precipitously, and Xe with a now very low Rn concentration is fed into the delay line. After the proper delay the Rn that was initially fed into the delay line when the reservoir still had all its Rn will emerge from the end of the delay line and mix with the by now essentially Rn free Xe in the reservoir. This raises the Rn concentration in the reservoir and therewith the Rn level of the Xe now entering the delay line. While the Rn level at the input to the delay line is thus rising, the very low Rn concentration that had previously entered it is still moving through the trap. Upon emerging from the trap into the Rn detector again this low concentration will start to lower the Rn concentration in the Rn detector again, giving rise to the damped oscillations observed in the onset of the measurements. Thus a sequence of lower and higher concentration mixes propagating through the delay line (trap) gives rise to the damped oscillations we see in the onset of our Rn concentration measurement cycles. Damping is effected by differentials in the propagation speed of Rn in the trap and mixing, with differentials in propagation speed arising from both diffusion and turbulence in the trap. As turbulence plays less of a role at lower Xe flow rates, the oscillations are more pronounced at lower flow rates. A measurement cycle ends when we raise the temperature of the trap to our 120 °C baking temperature and all the Rn adsorbed in the trap is released again, restoring the original Rn concentration in the system with its proper decline by decay. Isolating the trap and cooling it again or Xe recovery and trap modification prepares the system for a new measurement cycle.

Assuming that mixing in the Rn detector volume and flushing the thin 1/4 gas lines in the system is essentially instantaneous, the observed oscillation period becomes a direct measure of the Rn propagation speed  $v_{\text{Rn}}$  in the trap. With the Xe propagation speed given by the flow rate, we can then readily derive the ratio of the two.

Fig. 3 is zooming in on the start of the 0.50 l/min measurement cycle of the previous figure. For reference we also add the Rn concentration as traced by the  $^{214}\text{Po}$  decays in this figure. The time offset between the two traces is due to the longer lifetime of  $^{214}\text{Po}$  as compared to  $^{218}\text{Po}$ .

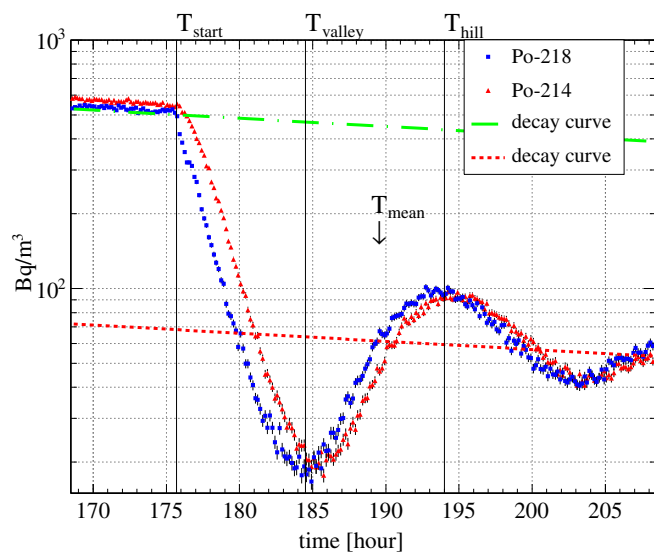


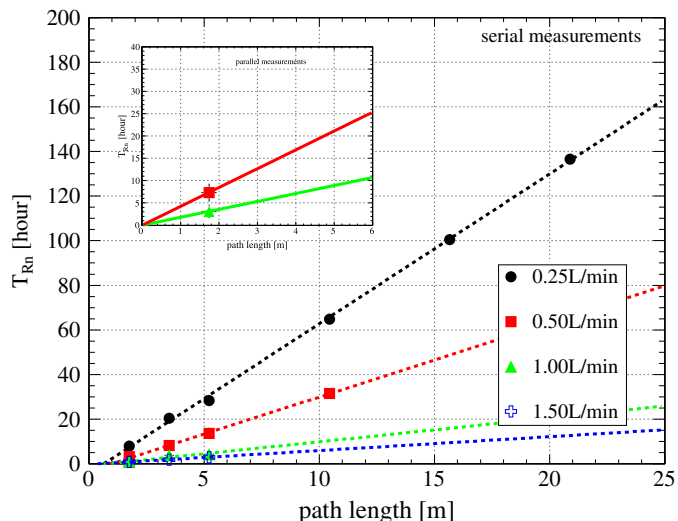
Fig. 3. Onset of Rn trapping for the 0.5 l/min sequence in Fig. 2. The squares are the same data points as in Fig. 2 and are derived from the  $^{218}\text{Po}$  counts in the Rn detector. The triangle data points are derived from the  $^{214}\text{Po}$  counts. Count rates for each data point are accumulated over 10 min. The meaning of the time labels (referenced to the  $^{218}\text{Po}$  curve) is explained in the text.

Also in Fig. 3 we marked four different times:  $T_{\text{start}}$  marks the time when the Rn concentration in the Rn detector starts to drop; this is the time when after re-inserting the now cold charcoal trap into the system and filling it with Xe from the Rn detector reservoir through the inlet to the trap the exit from the trap is opened to resume true circulation.  $T_{\text{valley}}$  and  $T_{\text{hill}}$  mark the first two extrema of the oscillatory part of the Rn concentration trace, and  $T_{\text{mean}} = (T_{\text{valley}} + T_{\text{hill}})/2$  is a point very close to the second zero crossing of the oscillating trace. In the more strongly damped high flow rate measurements shown at earlier times in Fig. 2 these are the only observable extrema, while in other measurements (see e.g. Fig. 7), where the Rn detector sensitivity became the limiting factor, sometimes only maxima are observable at all. Thus while the obvious choice for measuring the period of an oscillation would be to measure the time between its zero crossings we chose to measure it between extrema to better accommodate our data.

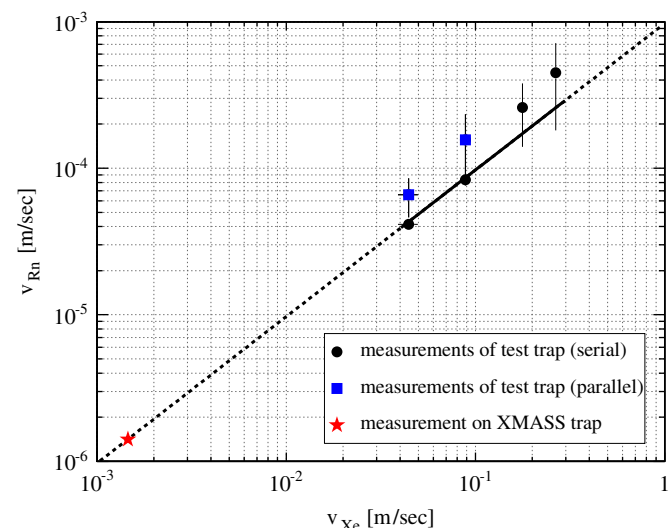
When interpreting our data we find that  $T_{\text{Rn}} = T_{\text{mean}} - T_{\text{start}}$  indeed measures the period of this oscillation, i.e. the mean time it takes Rn to move through the charcoal trap. This is verified on data where many oscillation periods are recorded, like the  $f_{\text{Xe}} = 0.25$  l/min data shown at late times in Fig. 2.

Fig. 4 summarizes the measurements of  $T_{\text{Rn}}$  as a function of the length of the charcoal trap. For each of the measured Xe flow rates the three measurement points up to trap lengths of 522 cm are simply the multiples of the fundamental length of 174 cm of each of our three traps. The measurement points at higher path length are obtained from the higher oscillations wherever they were reliably observable—i.e. at lower  $f_{\text{Xe}}$ . In line with our understanding of the oscillation mechanism each higher oscillation is interpreted as a renewed pass of a Rn concentration enhancement through the system, thus adding one more path through the charcoal trap. For the  $f_{\text{Xe}} = 0.25$  l/min data shown in Fig. 2 we were able to extract four oscillation periods, resulting in the three additional entries at multiples of the three trap serial combination's fundamental length of 522 cm. Thus Fig. 4 also validates our interpretation of the oscillation pattern.

Fig. 5 finally summarizes the  $v_{\text{Rn}}$  obtained from the fits of  $T_{\text{Rn}}$  vs. path length shown in Fig. 4. From the fit shown in this figure we extract  $v_{\text{Rn}}/v_{\text{Xe}}$  to be  $(0.96 \pm 0.10) \times 10^{-3}$  at a temperature of  $-85$  °C with our choice of Shirasagi G<sub>2X</sub> 4/6 for the charcoal traps.



**Fig. 4.**  $T_{Rn}$  as a function of the length of the trap. Dashed lines are fits to the data points for traps arranged in series at different flow rates, the solid line is for data points derived with two traps in parallel. Up to three traps could be arranged in series, and two in parallel. Entries for path lengths longer than the sum of real trap lengths are obtained by exploiting the oscillatory pattern to evaluate multiple passes through the existing traps.



**Fig. 5.** Mean propagation speeds for Rn vs. Xe. Circular data points come from the fits shown in Fig. 4, the star comes from the verification measurement on the trap designed for XMASS (Fig. 7). The line is constrained to go through the origin and fitted to the data points measured before the trap was designed for XMASS.

Also shown – but not used in the previous fit – is the result obtained with the Rn removal system designed for use in XMASS on the basis of above measurements, which will be discussed in the remainder of the paper.

### 3. Radon removal system design for the XMASS LXe detector

#### 3.1. System requirements

The XMASS detector in its current incarnation has a 700 l gas volume above and in equilibrium with its 1100 kg ( $\sim 380$  l LXe) of liquid that fill the whole of the detector volume in this single-phase experiment.

Great care was taken in choosing detector materials with respect to controlling the radioactivity emanating from all materials used in

the XMASS detector. From the pertinent measurements on the relevant materials we estimate that less than 12 mBq/700 l are emanating directly into the gas volume above the detector, originating mainly from the signal and high voltage cables of the PMTs. 12 mBq is also our upper limit estimate for emanation into the liquid, mainly coming from the PMT bases. If we achieve Rn reduction by a factor 10 or better in the gas, there should therefore be no noticeable addition to the activity in the detector from that source any more. At this level of 10% of background from the PMTs the remaining Rn would contribute of order  $10^{-5}$  dru to the overall background level in our fiducial volume.

With the half-life of  $^{222}\text{Rn}$  being 3.8 d, the  $T_{Rn}$  for Rn to stay in the trap must be longer than 12.7 days. Assuming a flow rate  $f_{Xe} = 1.00$  l/min  $= 1.7 \times 10^{-5}$  m<sup>3</sup>/s of gaseous Xe to be liquefied, a trade off between  $L_{trap}$  and  $A_{trap}$  can be made for this system and our choice of charcoal (Shirasagi G<sub>2X</sub> 4/6), but the volume of the system has to be

$$L_{trap}A_{trap} = f_{Xe} \frac{v_{Rn}}{v_{Xe}} T_{Rn} \geq 17\,560 \text{ cm}^3$$

using our measured value from above for  $v_{Rn}/v_{Xe}$ . This implies a total charcoal mass of more than 4.8 kg.

#### 3.2. System implementation

As the trap needs to be cooled, constraints on the dimensions of the system mainly come from the bath for the refrigerant and its insulation requirements. With an eye also to the flexibility a modular design offers, we chose to arrange two tubes of modest diameter in series, with enough room in the bath to add two more such tubes if needed. Each of these tubes is made from stainless steel, is 90 cm long, has an inner cross-sectional area of 113 cm<sup>2</sup>, and contains 2750 g of charcoal. Thus the two tubes amount to 5.5 kg of charcoal in the trap. To contain the charcoal and its dust and avoid contamination of the detector, the entrance and exit of each tube are sealed with a 0.003  $\mu\text{m}$  metal filter mesh.

A schematic view of the system is shown on the right hand side of Fig. 1. This figure also shows the locations of temperature sensors in and around one of the charcoal tubes in the trap. One measures the gas temperature at the inlet of the tube, while the other three measure its surface temperature from the outside. Around each tube a heating wire is wrapped to allow for baking of the tube and the charcoal contained in it. Fig. 6 shows different views of the system.

Given above system parameters and  $f_{Xe} = 1.00$  l/min we can calculate that  $v_{Rn}$  will be  $1.47 \times 10^{-3}$  m/s in the charcoal housings and for our system  $T_{Rn}$  becomes  $(14.74 \pm 1.60)$  days. This corresponds to 3.8 half-lives of  $^{222}\text{Rn}$  or an expected reduction by a factor of 1/14.6.

#### 3.3. System performance test

To verify the system performance the newly designed trap was installed into the circulation system as in Fig. 1, and Rn was introduced into the Xe again. As usual, the trap had been isolated under baking conditions, but then was cooled to  $-90$  °C for this test. While its intended operating temperature in XMASS detector is  $-100$  °C,  $-90$  °C is closer to the  $-85$  °C previously used to establish  $v_{Rn}/v_{Xe}$ . For those previous measurements the temperature was limited by the cooling system. During the test the temperature sensors indicated in Fig. 1 showed uniform readings within  $\pm 0.3$  °C even if warm Xe gas was circulated in the trap.

The results of this performance test are shown in Fig. 7. Despite a very high initial Rn concentration of 1000 Bq/m<sup>3</sup> at the start of the measurement cycle and integrating the Rn detector count rates over 12 h intervals the measurement was

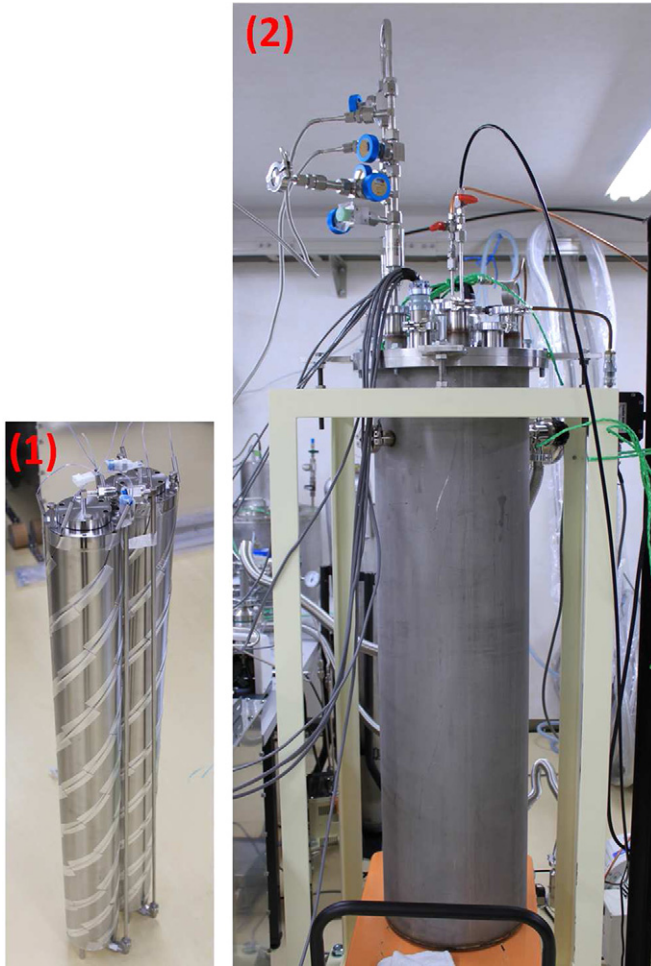


**Fig. 6.** Photographs of the Rn removal system for the XMASS. (1) is charcoal housings with heating wires. (2) is cryogenic system, which use pulse tube refrigerator and HFE as coolant.

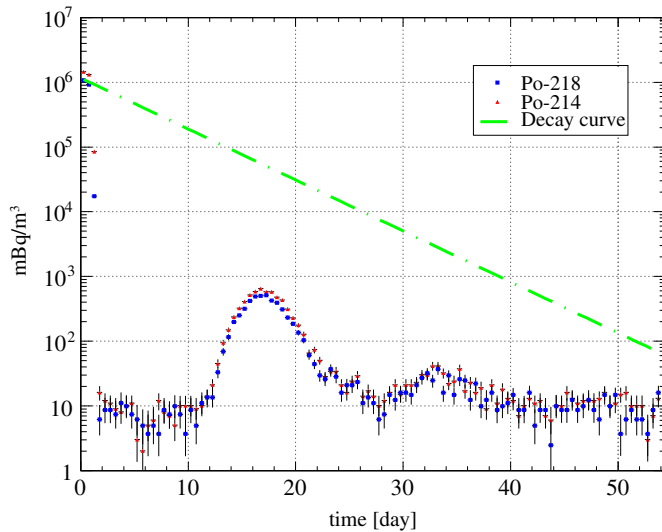


**Fig. 7.** The result of the Rn removal system test with 180 cm path length, 113 cm<sup>2</sup> cross-section. Data points are averaged over 12 h. Dashed spaced line is radon decay curve expected from initial radon value.

clearly limited by the sensitivity of our 70 l Rn detector. It cannot measure Rn concentrations less than 10 mBq/m<sup>3</sup>. Clearly visible are the initial fast reduction of Rn in the system, as well as the

first and second oscillation maximum. These allowed us to extract  $T_{Rn}$  again, which for this system evaluated to  $(14.75 \pm 0.50)$  days, which is in line with expectation—as evident in Fig. 5, where a star marks the measurement.

### 3.4. Measurement of radon emanation from system

Adding 5.5 kg of charcoal to a dedicated low background system, one concern has to be Rn emanation from the charcoal itself. However, the signal of Rn emanation from charcoal at low temperature is probably below the detection limit due to adsorption by charcoal itself. In order to make a conservative measurement of Rn emanation from the charcoal it has to be kept at baking temperature. For the high Rn concentrations artificially introduced for our previous measurements all Rn seems to be recovered from being trapped in the charcoal when the charcoal temperature is raised to 120 °C.

The emanation measurement was made after the new trap was installed to the circulation system of Fig. 1, and before any Rn was injected. To get a realistic result relevant for the intended operating conditions of the trap Xe was used as carrier gas for the measurement and circulated at a rate of 1.00 l/min. Since for this measurement we cannot artificially raise the Rn level, the integration time for each bin was increased from 10 min to 1 day, and instead of quoting Rn concentration we use the number of Rn decays directly.

Fig. 8 shows the result of this measurement. To interpret it we use the following equation:

$$\frac{dN(t)}{dt} = -\lambda N + \alpha_c + \alpha_{det} \quad (1)$$

where  $N(t)$  is the number of <sup>222</sup>Rn atoms in the Rn detector,  $\lambda$  is the <sup>222</sup>Rn decay constant, and  $\alpha_c$  and  $\alpha_{det}$  describe the emanation of <sup>222</sup>Rn from the charcoal and the Rn detector respectively. Here the term for the Rn detector is meant to include all system components other than the trap. The solution to this simple differential equation is

$$N(t) = \frac{\alpha_{tot}}{\lambda} (1 - e^{-\lambda t}) + N_0 e^{-\lambda t} \quad (2)$$

$$^{222}\text{Rn decay} = \alpha_{tot} (1 - e^{-\lambda t}) + \lambda N_0 e^{-\lambda t} \quad (3)$$

where  $N_0$  is the number of Rn atoms at the start of the measurement and  $\alpha_{tot} = \alpha_c + \alpha_{det}$ . The contribution from the  $N_0$  nuclei already

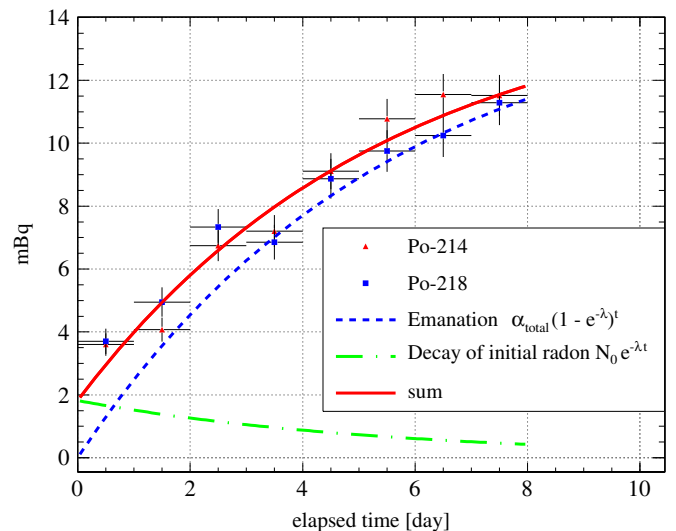


**Fig. 8.** The result of charcoal emanation measurement at baking temperature. Data points are averaged over 24 h. Dashed spaced line indicates decay of initial radon in the Rn detector. Dotted line shows emanated radon from charcoal and detector background. Solid line is sum of them.

present when the measurement starts will decay away, and ultimately a steady state will be reached where the number of Rn decays saturates at  $\alpha_{tot}$ .

The fit to the measured data is also shown in Fig. 8, as well as lines that show how the fit itself gets decomposed into the two terms contributing to it. The measured total emanation derived from this fit is  $(15.03 \pm 0.61)$  mBq, but it still contains the contribution from the Rn detector itself. In a background measurement during which pure Xe was circulated through the Rn detector bypassing the charcoal trap, this contribution was measured to be  $(4.54 \pm 0.20)$  mBq. This means that  $(10.49 \pm 0.64)$  mBq are emanating from the 5.5 kg of charcoal and its housing at 120 °C.

While the decay rate of  $^{226}\text{Ra}$  is independent of temperature, the dynamics of its daughter  $^{222}\text{Rn}$  emerging from the charcoal into the Xe gas surrounding it are likely to be altered at low temperature. In that sense we consider the measured value as an upper limit for the Rn emanation from our newly constructed charcoal trap. Assuming this worst case we next want to evaluate its impact on the trap's efficacy.

During operation, the newly emanating Rn will continually be added throughout the trap to the Rn that entered the trap with the circulating Xe, but unlike under the condition of the previous measurement (baking) the trap will now be cooled and adsorb its proper share of that mix. Using our above measured  $\nu_{Rn}$  in the trap we estimate the effect of uniform emanation along the length of our trap on the overall performance of the trap. We will assume that all the measured emanation originates exclusively from the charcoal and uniformly throughout the charcoal volume.

The emanation into a volume element  $A_{trap} dl$  at  $l$ , where  $l$  is the distance from the entrance to the trap, is  $\alpha_{c/g} \rho A_{trap} dl$ . Here  $\alpha_{c/g}$  is the emanation per unit mass of charcoal, and  $\rho$  is the density of charcoal averaged over the entire trap. The time it takes Rn at  $l$  to exit from the trap is  $(L_{trap}-l)/\nu_{Rn}$ , during which time a fraction of that Rn will decay, so that the surviving Rn is given as

$$\alpha_{c/dl} = \alpha_{c/g} \rho A_{trap} e^{-\lambda(L_{trap}-l)/\nu_{Rn}} dl. \quad (4)$$

Therefore, the total additional Rn output attributable to emanation from the charcoal in the trap integrates to

$$\begin{aligned} \alpha_{c/out} &= \int_0^{L_{trap}} \alpha_{c/g} \rho A_{trap} e^{-\lambda(L_{trap}-l)/\nu_{Rn}} dl \\ &= \alpha_{c/g} \rho A_{trap} \frac{\nu_{Rn}}{\lambda} (1 - e^{-\lambda(L_{trap}/\nu_{Rn})}). \end{aligned} \quad (5)$$

To simplify the expression Eq. (5) can be rewritten substituting  $A_{trap} = V/L_{trap}$ ,  $\rho V = M$ , and  $L_{trap}/\nu_{Rn} = T_{Rn}$ , as follows

$$\alpha_{c/out} = \frac{\alpha_{c/g} M}{\lambda T_{Rn}} (1 - e^{-\lambda T_{Rn}}) \quad (6)$$

where  $M$  is the total charcoal mass in the trap so that  $\alpha_{c/g} M$  becomes the total emanation from the charcoal, which above we measured to be  $10.49/5.5 = 1.91$  mBq/kg at baking temperature. Using  $T_{Rn} = 14.75$  day and  $M = 5.5$  kg, the total Rn output due to emanation from this trap is estimated to be  $\alpha_{c,out} \leq 3.1$  mBq. Note that ideally we would measure Rn emanation at low temperature, but trapping would further reduce the Rn available for measurement in a situation where already we are limited by the sensitivity of our Rn detector.

### 3.5. Expected effect on XMASS

Above we considered insertion of this trap into the gas line that takes gas from above the detector to liquefy it and thus compensate for evaporation from the liquid volume of the detector. This we refer to as gas–liquid circulation. If one wants to control the flow rate through the trap without artificially boiling off more liquid, lines exist to circulate Xe gas from above

the detector directly, which would be referred to as gas–gas circulation if no gas is liquefied in the process. Gas–gas and gas–liquid circulation can also coexist or be mixed.

For the purpose of this estimation we will consider the two possibilities separately. For gas–gas circulation the relevant volume is the 700 l Xe gas volume above the detector. With respect to this volume  $V$  the number of Rn atoms in it can be written as

$$\begin{aligned} \frac{dN(t)}{dt} &= -\lambda N(t) - \frac{f_{Xe}}{V} N(t) + \alpha_{gas} + \alpha_{c,out} + \beta(t) \frac{f_{Xe}}{V} N(t) \\ &= -\left\{ \lambda + \frac{f_{Xe}}{V} (1 - \beta(t)) \right\} N(t) + \alpha_{gas} + \alpha_{c,out} \end{aligned} \quad (7)$$

where  $\beta$  is the fraction of Rn that remains after passing through the trap. The first term describes Rn decay in the volume, the second the amount of Rn taken out with the Xe flow into the trap, the third  $\alpha_{gas}$  emanation from the detector materials in gas volume (e.g. cables), the fourth emanation from the charcoal trap, and the last the amount of Rn returned to the detector after the trap. If we assume the steady state, the  $\beta$  becomes constant, so that the solution to this equation is

$$N(t) = \frac{\alpha_{gas} + \alpha_{c,out}}{\gamma} (1 - e^{-\gamma t}) + N_0 e^{-\gamma t} \quad (8)$$

with  $\gamma = \lambda + (f_{Xe}/V)(1 - \beta)$ . Where  $N_0$  is the initial number of Rn. In the steady state solution the time dependent terms must vanish, and plugging in the measured values  $\beta = 1/14.6$ ,  $\alpha_{c,out} \leq 3.1$  mBq, and independently measured value  $\alpha_{gas} < 12$  mBq results in a total expected  $^{222}\text{Rn}$  activity  $< 1.3$  mBq/700 l for a Xe circulation flow of 1.00 l/min. As the detector's active volume is entirely in the liquid phase, it will be influenced by this measure only through the equilibrium that exists between the Rn concentrations in the liquid and gas phase, of which at this point we have little knowledge. As we would reduce the gas phase concentration, it should be expected that the liquid phase follows suit.

In the case of gas–liquid circulation the Rn leaving the trap would be added to the Rn in the detector's liquid (active) volume below the gas volume. As the liquid volume contains roughly 1100 kg of Xe it is rather large, and if we assume that no Rn returns from the liquid phase to the gas volume, the trap will essentially be used in a one-pass mode rather than in the re-circulation mode that is typical of the gas–gas operation. To estimate the impact of trap operation in this mode on the Rn concentration in the liquid volume we also assume that all Rn gets transferred into the liquid phase when we liquefy the Xe.

As far as the gas phase equations are concerned the trap outputs  $\beta(f_{Xe}/V)N(t)$  and  $\alpha_{c,out}$  are removed from the input side of the equation, which leads to

$$\frac{dN(t)}{dt} = -\left( \lambda + \frac{f_{Xe}}{V} \right) N(t) + \alpha_{gas}. \quad (9)$$

The solution now becomes

$$N(t) = \frac{\alpha_{gas}}{\delta} (1 - e^{-\delta t}) + N_0 e^{-\delta t} \quad (10)$$

with  $\delta = \lambda + (f_{Xe}/V)$ . Using the same values as quoted above for gas–gas circulation, the steady state  $^{222}\text{Rn}$  activity in the gas volume is expected to become  $< 1.00$  mBq/700 l, lower than in the gas–gas circulation case.

In the liquid volume though the only means to dispose of Rn is through its decay. This has to be in equilibrium with the inputs, which now consist of the Rn that passes through the trap from its input in the gas volume, Rn emanation in the trap, and emanation  $\alpha_{liq}$  from the detector into the liquid volume

$$\frac{dN_{liq}(t)}{dt} = -\lambda N_{liq}(t) + \beta \frac{f_{Xe}}{V} N_{gas}(t) + \alpha_{c,out} + \alpha_{liq} \quad (11)$$

where  $N_{gas}(t)$  is given by Eq. (10), and it becomes  $\alpha_{gas}/\delta$  for the steady state. Plugging in above numbers the Rn activity in the liquid volume now becomes  $(4.83 + \alpha_{liq})$  mBq/1100 kg, where we restricted the LXe mass to the portion that is contained in the active volume of the detector.

Clearly Rn activity in the gas volume can be reduced by means of gas–gas circulation through this newly designed charcoal trap. If a stronger reduction of the Rn concentration in the gas phase is desired, the modular design allows for easy doubling of the trap length which could be combined with an increased flow rate.

Rn activity in the liquid volume on the other hand is directly affected by  $\alpha_{c,out}$  so that cleaner charcoal would be needed to further reduce Rn. If on the other hand Rn emanation from our charcoal at low temperature is different from what we measured at baking temperature, the trap might even perform better than expected.

#### 4. Conclusion

The efficient removal of Rn contamination from Xe gas using activated charcoal was demonstrated and can be understood in analogy to the passing of gases through a column in a gas chromatograph. In this picture it is the slower propagation of Rn relative to Xe in combination with the 3.8 d half life of the longest lived Rn isotope that allows for efficient removal if the “column” is long enough for a sufficient fraction of the Rn to decay before it re-emerges from the column. For our choice of charcoal (Shirasagi G<sub>2x</sub> 4/6) we measured  $v_{Rn}/v_{Xe} = (0.96 \pm 0.10) \times 10^{-3}$ .

Building on these measurements we designed a Rn removal trap for the XMASS detector itself. Its design performance with respect to Rn retention for  $14.75 \pm 0.50$  d at a 1.00 l/min Xe flow

rate was verified and the system is ready for deployment in XMASS. At the above flow rate and with our conservative upper limit calculation for the Rn emanation from detector materials assuming an initial Rn activity in the gas volume of 12 mBq we would expect to achieve the following improvement after deployment in XMASS: gas–gas circulation should reduce the Rn activity in the gas to 7% of its original value from 12 mBq to 1.3 mBq per 700 l. Gas–liquid circulation should reduce the Rn transfer into the liquid by a factor of 0.4 from 12 mBq to 4.8 mBq.

#### Acknowledgments

We gratefully acknowledge the cooperation of Kamioka Mining and Smelting Company. This work was supported by the Japanese Ministry of Education, Culture, Sports, Science and Technology, and Grant-in-Aid for Scientific Research.

#### References

- [1] Y. Suzuki, et al., ICRR-Report-465-2000-9, hep-ph/0008296.
- [2] E. Aprile, et al., Physical Review Letters 105 (2010) 131302.
- [3] D.S. Leonard, et al., Nuclear Instruments and Methods in Physics Research A 591 (2008) 490.
- [4] A. Minamino, et al., arXiv:0912.2405.
- [5] K. Abe, et al., Astroparticle Physics 31 (2009) 290.
- [6] K. Munakata, et al., Journal of Nuclear Science and Technology 36 (1999) 818.
- [7] S. Fukuda, et al., Nuclear Instruments and Methods in Physics Research A 501 (2003) 418.
- [8] M. Ikeda, et al., Radioisotopes 59 (2010) 29.
- [9] S. Maurer, et al., Chemical Engineering Science 56 (2001) 3443.
- [10] H. Simgen, AIP Conference Proceedings 785 (2004) 121.
- [11] Y. Takeuchi, et al., Nuclear Instruments and Methods in Physics Research A 421 (1999) 334.
- [12] <<http://www.apinet.co.jp/pdgetter.html>>.